JOURNAL OF MATERIALS SCIENCE 23 (1988) 1739–1744

The occurrence of a new metastable phase in an Al–6.8 at % Zn alloy

R. RAMLAU, H. LÖFFLER
Pädagogische Hochschule Halle, Sektion Mathematik/Physik, Kröllwitzer Straße 44, DDR-4050 Halle (Saale), GDR

Evidence for the occurrence of a hitherto unknown metastable phase (β_m) is found by lattice fringe imaging an Al–6.8 at. % Zn alloy aged at 120° C for about 4 days. Additional information is obtained by the analysis of Moiré fringes related to the precipitates of the β_m phase. It is suggested that the novel phase has an h c p structure with $a^{hex} = 0.274$ nm and $c^{hex} = 0.450$ nm as the lattice parameters. The ratio $c^{hex}/a^{hex} = 1.64$, which corresponds to an almost ideal h c p structure. The possibility of whether β_m precipitates can form directly from large ellipsoidal Guinier–Preston zones or small precipitates of the rhombohedral α'_R phase is discussed.

1. Introduction

In the past fifteen years high resolution electron microscopy (HREM) has developed into a greatly appreciated means of studying the early stages of decomposition in age-hardenable aluminium alloys. Parsons *et al.* [1] were the first to apply lattice fringe imaging to the investigation of Guinier–Preston (GP) zones in Al–Cu alloys. Later, Lyman and Van Der Sande [2], as well as the present authors [3], succeeded in lattice fringe imaging of GP zones in Al–Zn–Mg and Al–Zn alloys, respectively.

The Al–Zn system became the subject of more and more extended basic research, and it is nowadays widely considered one of the best studied binary systems. Its outstanding importance arises from some favourable circumstances allowing the scientist to investigate a large variety of those fundamental processes with which physical metallurgy is concerned.

Particular interest has been shown in the study of aluminium-rich Al–Zn alloys, which are most suitable for investigation of the mechanisms and kinetics of phase transformations in supersaturated solid solutions. In these alloys, continuous decomposition of the supersaturated, and therefore unstable, f c c mixed-crystal cannot proceed by direct precipitation of the h c p β equilibrium-phase, except by heterogeneous nucleation. In general, the mid-grain regions are lacking in nucleation sites for this phase, and the β precipitation is preceded by sequential precipitation of metastable phases.

In the middle of the sixties it became obvious [4–6] that in Al–Zn alloys with zinc contents between 9 and 15 at. % the precipitation sequence at elevated ageing temperatures, e.g. at $T_a = 180°$ C, is: spherical GP zones → ellipsoidal GP zones → rhombohedral α'_R phase → f c c α'_m phase → β equilibrium phase. Later it was proved that this full sequence may be shortened according to the ageing temperature applied [7–10].

The general features of structure changes associated with the successive transformations in a more stable phase are known; many details, however, remained unclear. Thus, a few years ago we began a study of the mechanisms of structure changes in an Al–6.8 at.% Zn alloy by lattice fringe imaging. If this alloy is aged at $T_a = 120°$ C, a shortened sequence is expected, i.e. spherical GP zones → ellipsoidal GP zones → α'_R phase → β phase. Only the α'_m phase is missing. It was shown that the ellipsoidal GP zones lose their full coherency with the ambient matrix when growing to a certain size and that only this breakdown of the full coherency marks the transition of GP zones into the precipitates of the (semicoherent) α'_R phase [11, 12]. The size/shape relation of growing zones and small α'_R precipitates was also established [13].

In the course of these investigations, the occurrence of a metastable phase, hitherto not mentioned in the literature, has been observed. It is the objective of this paper to report both the structure of this phase and the supposed mechanism of its formation.

2. Experimental procedure

2.1. Electron microscopy

The application of HREM to the analysis of precipitates is rather limited. Lattice fringe imaging requires very thin specimens, the thickness of which should be equal to one-quarter, or three-quarters at most, of the corresponding extinction distance ξ_g. The more sophisticated techniques of HREM, e.g. structure imaging, require even thinner specimens.

Using a 100 kV electron microscope, as in this study, {1 1 1} lattice fringes in pure aluminium will be imaged with maximum contrast if the specimen is $\frac{1}{4}\xi_g = 14$ nm thick. If the thickness is $\frac{3}{4}\xi_g$, a diminution of the lattice fringe contrast must be accepted, and further increasing the thickness makes lattice fringe imaging impossible.

Because it is always difficult to prepare very thin and smooth foils from binary systems containing precipitates (because of selective etching, etc.) and as it is sometimes considered necessary that the precipitate under investigation is still entirely surrounded by matrix material, HREM investigations of larger

0022–2461/88 $03.00 + .12

precipitates (> 45 nm) can hardly be carried out with 100 kV instruments. Using instruments with higher acceleration voltages makes the situation a little more positive, but even then structure imaging is restricted to the earliest products of decomposition, e.g. GP zones in Al–Cu alloys [14].

The micrographs presented here have been taken in the JEM-100C microscope (acceleration voltage $U_a = 100$ kV) by employing two-beam lattice fringe imaging with tilted illumination, because in the two-beam tilted mode the resolving power of the microscope with respect to lattice fringes is higher than in the axial mode. Using the standard stage of the JEM-100C, the spherical aberration constant amounted to $C_s = 1.4$ mm.

The lattice fringe distances were measured on the photographic plates by means of an Abbe comparator.

Finally, it seems worth mentioning that there are serious objections to the reliability of lattice fringe imaging of crystal defects, e.g. dislocations. Such objections, however, are not relevant if rather large precipitates are imaged, the crystal structure of which sufficiently differs from that of the matrix, and if their analysis is based upon the fringe distances as well as on the angles between various sets of fringes. For those who wish to enter into detail concerning theory and practice of HREM, a monograph by Spence [15] is recommended.

2.2. Specimen preparation

Samples of the Al–6.8 at. % Zn alloy produced from high-purity (99.99%) components, were carefully homogenized and gradually rolled to sheets of about 0.15 mm thick. These sheets were homogenized again (1 h at 400° C), quenched in an oil-bath at an ageing temperature $T_a = 120°$ C and stored there for a certain time. Thin foils were obtained by electropolishing (window technique) at about $-15°$ C, using an electrolyte mixed from 400 ml absolute methyl alcohol, 125 ml absolute ethyl alcohol, 300 ml ethylene glycol, and 25 ml perchloric acid (60%).

3. Results and discussion

Ageing the samples for about 4 days at $T_a = 120°$ C yielded precipitates like those shown in Figs 1 and 2. The lattice fringes inside the precipitates are distinctly inclined to the matrix fringes and have different spacings. Moreover, the precipitates display strong Moiré fringes.

Moiré fringes arise from interference caused by sets of lattice planes of the matrix and the precipitate, respectively. They may be analysed by means of the well-known formulae

$$D = \frac{d_m d_p}{(d_m^2 + d_p^2 - 2d_m d_p \cos\phi)^{1/2}}$$

$$\sin\beta = \frac{d_m \sin\phi}{(d_m^2 + d_p^2 - 2d_m d_p \cos\phi)^{1/2}} \quad (1)$$

where d_m and d_p are the spacings of interfering lattice planes in the matrix and the precipitate, respectively, ϕ is the angular rotation between these two sets of lattice planes, D the spacing of the Moiré fringes, and β the angle between the Moiré fringes and the relevant lattice fringes of the matrix.

The new precipitates resemble ellipsoidal GP zones and smaller precipitates of the α'_R phase in size, shape, and their arrangement within the matrix crystal [13]. They are in the shape of an oblate spheroid with its polar axis parallel to one of the four $\langle 1\,1\,1\rangle$ directions of the fcc matrix, i.e. with its equatorial plane placed in one of the $\{1\,1\,1\}$ matrix planes. The mean radius, r_m, of a precipitate is often defined to be the radius of a sphere equal in volume. If the lengths of the major and the minor semi-axis are referred to as A and C, respectively, $r_m = (A^2C)^{1/3}$ holds for oblate spheroids. Note that the semicoherent α'_R precipitates with $r_m \approx 10$ nm as well as the precipitates of Figs 1 and 2

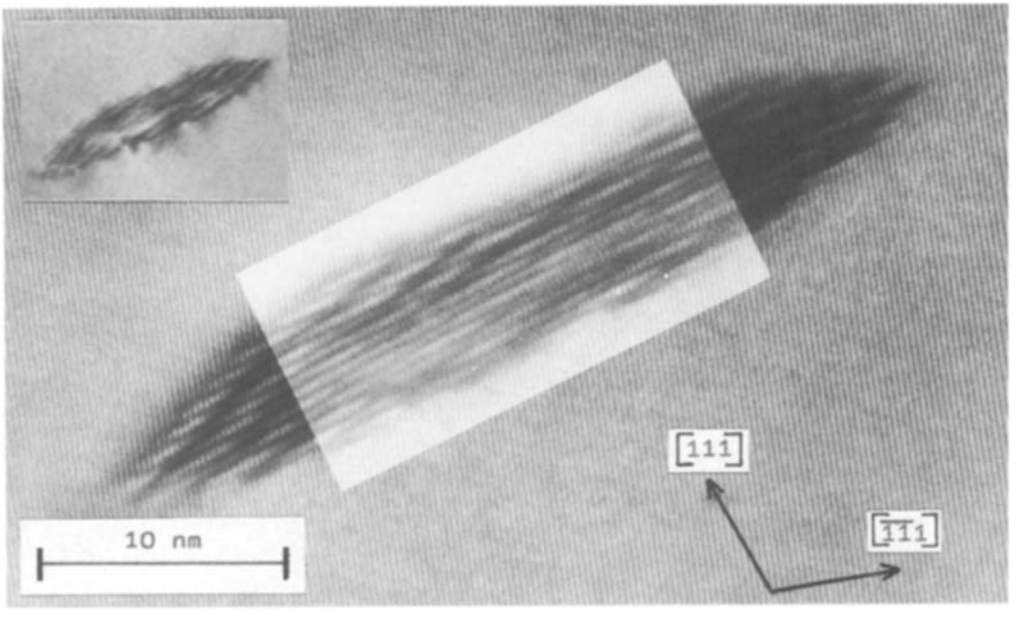

Figure 1 Ellipsoidal precipitate of the β_m phase and $(\bar{1}\,\bar{1}\,1)^{cub}$ planes in the matrix. Inside the precipitate hexagonal (0 1.0) planes with $d = 0.237$ nm are imaged as well as two types of Moiré fringes. For the sake of perceptibility, a rectangular region in the centre has been shaded in the photographic reproduction. The lattice fringes and the Moiré patterns are shown schematically in Fig. 3. Foil orientation $[\bar{1}\,1\,0]$; ageing time 5 days.

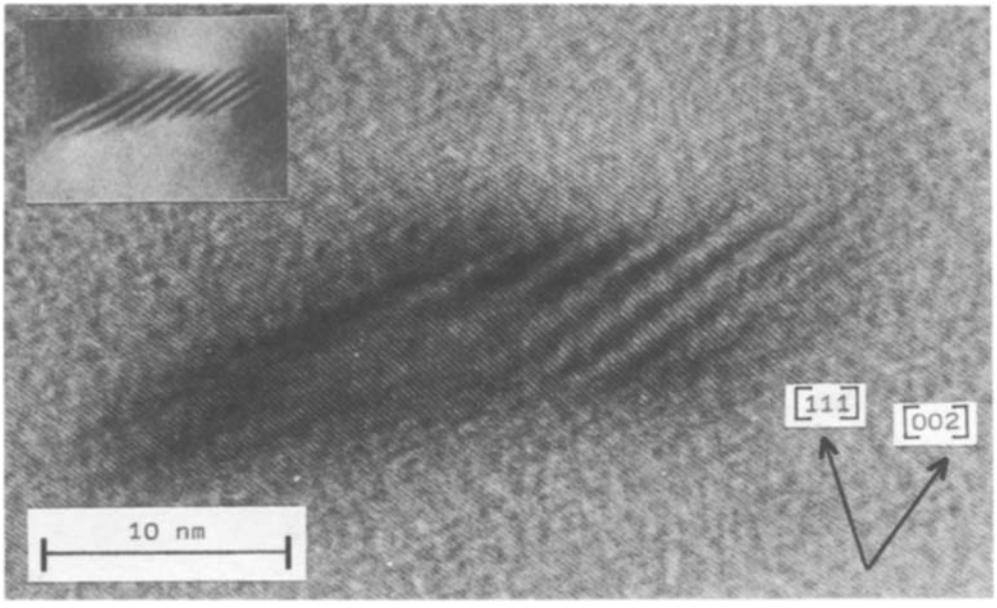

Figure 2 Ellipsoidal precipitate of the β_m phase and $(0\,0\,2)^{cub}$ planes in the matrix. Inside the precipitate hexagonal (0 1.1) planes with $d = 0.211$ nm are imaged as well as Moiré fringes due to the interference of $(0\,0\,2)^{cub}$ and (0 1.1) planes. Foil orientation $[\bar{1}\,\bar{1}\,0]$; ageing time 68 h.

are most precisely described as lenticular. Nevertheless, the spheroidal shape remains a very good approximation when determining the volume of these precipitates.

Considering the results of the former lattice fringe studies [11, 12] it becomes evident that the crystal lattice of the new precipitates is different from that of ellipsoidal GP zones and the α'_R phase. The lattice of the two latter phases is rhombohedrally distorted fcc, and for the sake of clarity it is often described on the basis of a face-centred rhombohedral unit cell. One can imagine this unit cell as being originated by compression of the fcc unit cell in one of its body diagonals (cubic $\langle 1\,1\,1\rangle$ direction). Furthermore, the edge length of the rhombohedral unit cell is slightly smaller than that of the fcc cell. Thus the orientation relationship between precipitate and matrix is:

$$(1\,1\,1)^{rh} \parallel (1\,1\,1)^{cub}$$

$$[\bar{1}\,\bar{1}\,2]^{rh} \parallel [\bar{1}\,\bar{1}\,2]^{cub}$$

(Of course, the rhombohedral $[1\,1\,1]^{rh}$ direction coincides with the polar axis of the oblate spheroids mentioned above.) As the atomic radii of aluminium and zinc differ only slightly, the rhombohedral distortion of the precipitate lattice is rather weak, even if the precipitates contain up to about 70 at. % Zn.

From lattice fringe micrographs $[1\bar{2}]$ of both ellipsoidal GP zones and α'_R precipitates nucleated and grown at $T_a = 120°\,C$, and therefore containing about 65 at. % Zn, the following lattice parameters were obtained for precipitate sizes of $r_m \approx 8$ to 9 nm

$$a^{rh} = (0.3985 \pm 0.0005)\,nm$$

$$\alpha^{rh} = 91.1° \pm 0.01° \qquad (2)$$

For comparison, the cubic lattice parameter of the zinc-depleted matrix is $a^{cub} = 0.4050$ nm.

As the resulting misfit in lattice spacings, as well as the lattice rotations, are too small, the drastic effects demonstrated in Figs 1 and 2 cannot be explained on the basis of the rhombohedrally distorted fcc lattice. It should be emphasized that in the case of ellipsoidal GP zones and small α'_R precipitates ($r_m \approx 8$ nm), in principle, no Moiré patterns can be observed. Consequently, the novel precipitates are easy to discriminate from the other ellipsoidal or lenticular precipitates seen in the microscope.

Furthermore, one might suppose that the reported sequence of structure changes is not valid for the special thermo-mechanical treatment applied in this work, and thus the fcc α'_m phase can form at the expense of the α'_R phase. This, however, can be excluded for three reasons.

(1) The spacing of fringes visible inside the precipitate of Fig. 1 is slightly larger than all the spacings occurring in the fcc α'_m phase, with $d_{\{1\,1\,1\}} = 0.231$ nm being the largest.

(2) As proved, for example, by Werner and Löffler [16], there is a certain orientation relationship between the fcc matrix and the fcc α'_m lattice. Equally indexed lattice planes of the matrix and the precipitate, respectively, are never rotated against each other by more than 1°.

(3) It is well established that the shape of α'_m precipitates is spherical or globular rather than ellipsoidal or lenticular.

We will now test whether the lattice fringes inside the novel precipitates may be interpreted on the basis of an hcp structure. Figs 1 and 2 show equisized lenticular precipitates of mean radius $r_m \approx 10$ nm. The lattice fringes visible in the matrix are $(\bar{1}\,\bar{1}\,1)^{cub}$ and $(0\,0\,2)^{cub}$ planes, respectively, with $d^{cub}_{(\bar{1}\,\bar{1}\,1)} = 0.234$ nm and $d^{cub}_{(0\,0\,2)} = 0.202$ nm. As Fig. 1 is a little confusing, its general features are shown schematically in Figs 3 and 4. The lattice fringes inside the precipitate are exactly parallel to the $(\bar{2}\,\bar{2}\,4)^{cub}$ matrix planes, which are not imaged (cf. scheme a in Fig. 3), and have a spacing of (0.237 ± 0.002) nm. This is an additional indication that these lattice fringes cannot in any way be associated with ellipsoidal GP zones or α'_R precipitates,

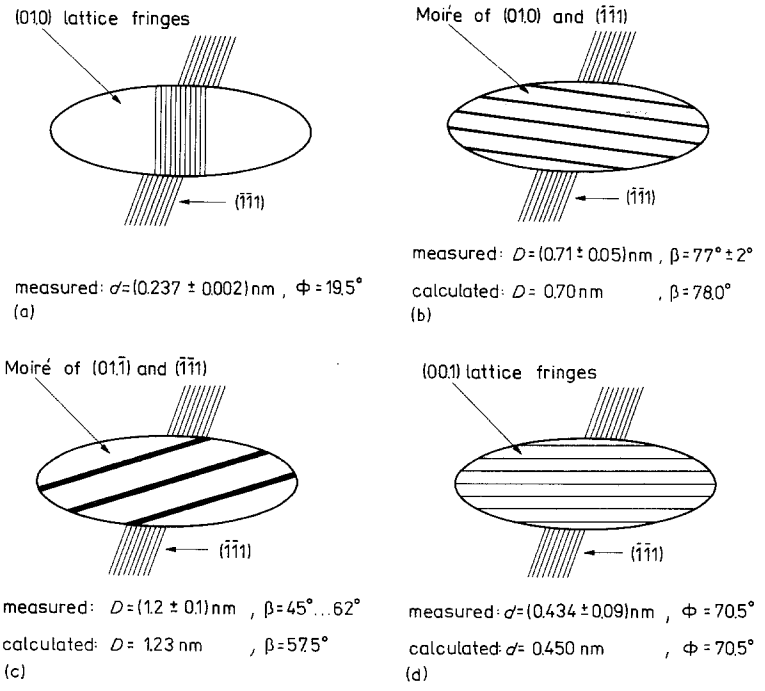

Figure 3 Schematic illustration of the main features of Fig. 1. The measured values of spacings and angles are compared with those values calculated with the lattice parameters (Equation 6) and Equation 1. D and d are the spacings of Moiré fringes and lattice frinces, respectively, ϕ is the angle between lattice planes of the matrix and the precipitate, and β is the angle between the Moiré fringes and the matrix planes. The originally forbidden (0 0.1) fringes in (d) arise from double refraction.

because Equation 2 results in $d^{rh}_{(2\bar{2}4)} = 0.084\,nm$, which is only about 30% of the measured value.

On the basis of the well-known orientation relationship

$$\begin{aligned}(0\,0.1) &\parallel (1\,1\,1)^{cub}\\ [0\,1.0] &\parallel [\bar{1}\,\bar{1}\,2]^{cub}\end{aligned} \tag{3}$$

which is also valid for the β equilibrium-phase, the precipitate fringes in Fig. 1 must be identified with hexagonal (0 1.0) planes, hence

$$d_{(0\,1.0)} = (0.237 \pm 0.002)\,nm \tag{4}$$

can be derived.

It has never been possible to observe particular (0 0.2) lattice fringes, either in specimens with $[\bar{1}\,\bar{1}\,0]$ orientation or with other orientations, allowing the lenticular precipitates to be imaged edge-on. In other words, imaging $(1\,1\,1)^{cub}$ matrix-planes all the precipitates under consideration looked like ellipsoidal GP zones or α'_R precipitates. Therefore it seems reasonable to suppose that $d_{(00.2)} = d^{rh}_{(1\,1\,1)}$.

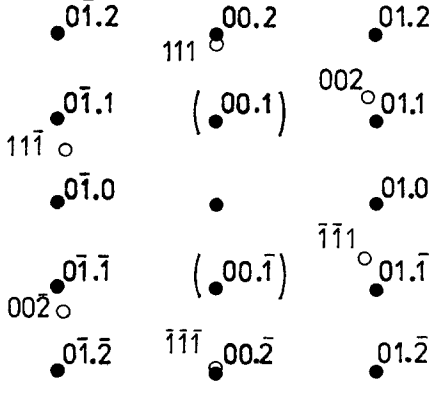

Figure 4 Diagram of the relationship between (●) the precipitate and (○) the matrix diffraction patterns for Figs 1 and 2. Matrix orientation $[\bar{1}\,1\,0]$.

From Equation 2 or the values directly measured [11, 12] it follows that

$$d_{(00.2)} = (0.225 \pm 0.001)\,nm \tag{5}$$

Equations 4 and 5 give rise to the hexagonal lattice parameters

$$\begin{aligned}a^{hex} &= (0.274 \pm 0.003)\,nm\\ c^{hex} &= (0.450 \pm 0.002)\,nm\end{aligned} \tag{6}$$

which are quite different from those of the β phase that consists of almost pure zinc [17]

$$\begin{aligned}a^{hex} &= 0.2665\,nm\\ c^{hex} &= 0.4947\,nm\end{aligned} \tag{7}$$

In a future paper, we [18] will show that the lattice parameters (Equation 7) of the stable β phase need to be corrected slightly, at least if this phase precipitates in an Al–6.8 at. % Zn alloy at $T_a = 120°C$. But this correction is of no importance to the discussion given here.

On the basis of the orientation relationship (Equation 3) and the lattice parameters (Equation 6) derived above, all the experimental data concerning lattice fringes and Moiré fringes may be entirely understood within the frame of experimental error.

In Fig. 2, for example, the precipitate fringes are then (0 1.1) fringes. Their spacings amount to (0.211 ± 0.002) nm and their angle with the $(0\,0\,2)^{cub}$ matrix fringes is 7.5° ± 0.5°. Taking, on the other hand, the parameters in Equation 6, $d_{(0\,1.1)} = 0.210\,nm$ and $\phi = 7.5°$ are calculated. Of course, the Moiré fringes in Fig. 2 arise from interference of (0 1.1) and $(0\,0\,2)^{cub}$ planes. (See also Fig. 4.)

Using other orientations which allow the lenticular precipitates to be imaged edge-on, imaging of hexagonal lattice fringes inside the precipitates failed. But

this negative result is fully consistent with the model based on Equations 3 and 6. Taking for example, a specimen of $[\bar{1}\,\bar{1}\,2]$ orientation, one would expect $[\bar{2}\,1.0]$ lattice fringes lying parallel to the polar axis of the edge-on precipitates. From Equation 6 $d_{(\bar{2}\,1.0)} = 0.137\,\text{nm}$ is derived, which is beyond the resolution power of the microscope used for this study.

It seems worth mentioning that Moiré fringes from (0 0.2) and $(1\,1\,1)^{cub}$ (cf. Fig. 4) have never been observed. This rather astonishing fact is because of the relatively small "thickness" ($2C$) of the lenticular precipitates, which is only 6 to 8 nm. Taking the lattice spacings given above and modifying Equation 1 for the case of parallel Moiré fringes ($\phi = 0$) one obtains $D = 5.85\,\text{nm}$. Obviously this value is too high to generate a set of Moiré fringes. This finding is in full accordance with earlier investigations concerning ellipsoidal GP zones α'_R precipitates of $r_m \approx 10\,\text{nm}$ [11, 12].

It has been demonstrated above that the precipitates imaged in Figs 1 and 2 can neither be associated with the metastable phases known nor with the stable β phase. That is why they should be regarded as precipitates of a metastable phase, which is designated β_m.

It is suggested that the β_m phase has an h c p structure with an orientation relationship given in Equation 3 and with the lattice parameters of Equation 6. Thus the β_m phase distinguishes itself by its almost ideal h c p structure with $c^{hex}/a^{hex} = 1.64$, whereas $c^{hex}/a^{hex} = 1.856$ holds for the β phase consisting of pure zinc. Although the experimental results reported in this study are in conformity with the suggested structure, a regular and fully satisfying structure analysis should be the subject of future investigations by X-ray analysis or improved HREM methods.

As already outlined, large ellipsoidal GP zones, small α'_R precipitates, and β_m precipitates are equal in both size and shape. In addition, not only (0 0.1) $\parallel$ $(1\,1\,1)^{cub}$ holds, but also $d_{(0\,0.2)} = d^{rh}_{(1\,1\,1)}$. The formation of the β_m phase is therefore supposed to proceed via a direct structure change within the ellipsoidal GP zones or α'_R precipitates, i.e. by a martensitic transformation from the rhombohedrally distorted f c c lattice into the h c p lattice. This kind of transformation is associated with the formation of a stacking fault in a $(1\,1\,1)^{rh}$ plane and the successive shear of every other $(1\,1\,1)^{rh}$ plane (see, for example, [19]). The initial stacking fault, for its part, may be caused by the splitting of matrix dislocations or by the condensation of interstitial atoms on the close-packed planes.

As the transition of fully coherent ellipsoidal GP zones into semicoherent α'_R precipitate is most likely induced by the condensation of interstitial atoms on $(1\,1\,1)^{rh}$ or $\{\bar{1}\,\bar{1}\,1\}^{rh}$ planes [12], the formation of the β_m phase may be due to an anomalous course of this coherency loss. The precipitation sequence would then be

ellipsoidal GP zones → α'_R
ellipsoidal GP zones → β_m

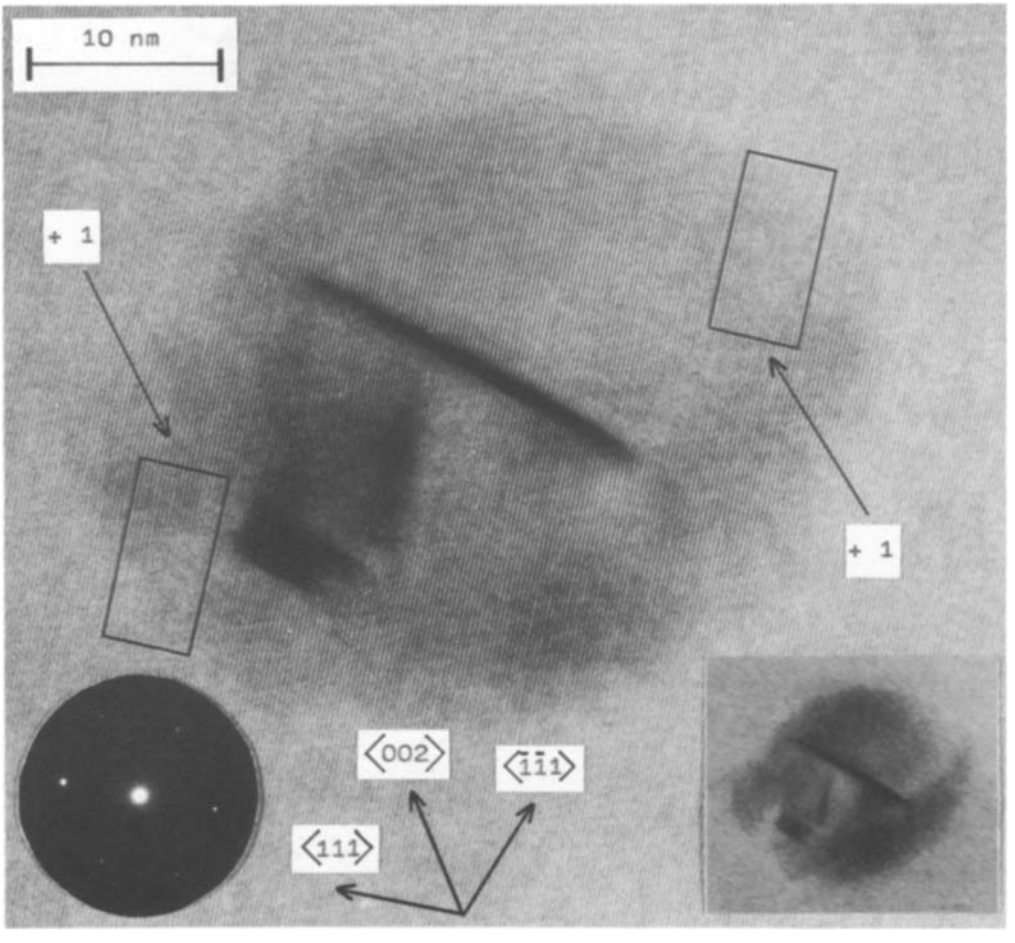

Figure 5 Ellipsoidal precipitate, imaged almost flat-on, and matrix planes of type $\{1\,1\,1\}^{cub}$ with $d = 0.234\,\text{nm}$. Inside the precipitate three stacking faults or microlamellae of the h c p structure are seen on planes of type $\{\bar{1}\,\bar{1}\,1\}^{rh}$, two of which are imaged edge-on. Foil orientation $\langle 1\,\bar{1}\,0\rangle$ type; ageing time 5 days.

In general, the extra $(1\,1\,1)^{rh}$ or $\{\bar{1}\,\bar{1}\,1\}^{rh}$ planes are surrounded by glissile dislocation loops of Burgers vector $\boldsymbol{b} = \frac{1}{2}a^{cub}\langle 1\,1\,0\rangle$, which means the resulting semicoherent α'_R precipitates are free of stacking faults. Under certain conditions, however, the condensation of interstitial atoms on $(1\,1\,1)^{rh}$ or $\{\bar{1}\,\bar{1}\,1\}^{rh}$ planes may be connected with the formation of stacking faults. This is supported by Fig. 5, which shows an ellipsoidal or lenticular precipitate, imaged almost flat-on, with three stacking faults or microlamellae of h c p structure on planes of type $\{\bar{1}\,\bar{1}\,1\}^{rh}$, two of which are seen edge-on. Amelinckx [18] shows these defects are to serve as nucleation sites for the stable β phase. The martensitic transformation suggested above and, accordingly, the formation of the β_m phase, are expected to proceed only if the initial stacking fault lies on a $(1\,1\,1)^{rh}$ plane, i.e. in the equatorial plane of the precipitates.

Taking into account that it has never been possible to observe the formation of β_m precipitates *in situ*, the precipitation sequence ellipsoidal GP zones $\rightarrow \alpha'_R \rightarrow \beta_m$ cannot be excluded.

As a consequence of the direct structure transformation, the β_m phase should have almost the same zinc content as its predecessors, i.e. about 65 at. %. On the other hand, the stable β phase contains almost 100 at.% Zn. This difference in the zinc content explains the striking differences between the lattice parameters of these two h c p phases.

One should note that there is no strain field around the β_m precipitates. They are incoherent or, perhaps, semicoherent. In any case the degree of their coherency is still lower than that of the semicoherent α'_R phase.

Eventually it should be stressed that β_m precipitates occurred rather seldom. This is probably the reason why the β_m phase has not yet been discovered by X-ray methods. It must also be considered possible that the β_m phase forms only in thin foils and not in bulk material.

Acknowledgement

The micrographs presented in this paper were taken in the JEM-100 C electron microscope in the Institute of Solid State Physics and Electron Microscopy of the Academy of Sciences of the GDR in Halle. The authors are grateful to the head of this institute for permitting the use of this instrument.

References

1. J. R. PARSONS, M. RAINVILLE and C. W. HOELKE, *Philos. Mag. Ser. 8* **21** (1970) 1105.
2. C. E. LYMAN and J. B. VAN DER SANDE, *Metall. Trans.* **A7** (1976) 1211.
3. R. RAMLAU and H. LÖFFLER, *Phys. Status Solidi (a)* **68** (1981) 531.
4. W. MERZ and V. GEROLD, *Z. Metallkde* **57** (1966) 607.
5. M. SIMERSKA and V. SYNECEK, *Acta Metall.* **15** (1967) 223.
6. G. J. C. CARPENTER and R. D. GARWOOD, *Metal Sci. J.* **1** (1967) 202.
7. M. SIMERSKA and V. SYNECEK, *Acta Crystallogr.* **A31** (S3) (1975) 185.
8. *Idem, ibid.* **A34** (S4) (1978) 304.
9. M. SIMERSKA and P. BARTUSKA, *Czech. J. Phys.* **B24** (1974) 77.
10. *Idem, ibid.* **B27** (1977) 655.
11. R. RAMLAU and H. LÖFFLER, *Crystal Res. Technol.* **19** (1984) 1279.
12. *Idem, ibid.* **21** (1986) 453.
13. *Idem, Phys. Status Solidi (a)* **79** (1983) 141.
14. D. DORIGNAC, M. J. CASANOVE, R. JAGUT and B. JOUFFREY, in "Electron Microscopy 1980", Vol. 4, edited by P. Brederoo and J. van Landuyt (Leiden, 1980) p. 174.
15. J. C. H. SPENCE, "Experimental High-resolution Electron Microscopy" (Clarendon, Oxford, 1980).
16. M. WERNER and H. LÖFFLER, *Crystal Res. Technol.* **18** (1983) 459.
17. C. BARRETT and T. B. MASSALSKI, "Structure of Metals" (Pergamon, Oxford, 1980).
18. R. RAMLAU and H. LÖFFLER, *Acta Metall.* **35** (1987) 2005.
19. S. AMELINCKX, in "Dislocations in Solids", Vol. 2, edited by F. R. N. Nabarro (North-Holland, Amsterdam, 1970) p. 88.

Received 24 July 1986
and accepted 17 August 1987